

Contactless Breathing Airflow Detection on Smartphone

Wei Liu^{ID}, Shan Chang^{ID}, Member, IEEE, Feng Li, Yong Xu, Shizong Yan, and Ye Liu

Abstract—Accurate and continuous breathing rate detection is crucial as it can help people to assess their physical health and provide early warning and diagnosis for potential human diseases. Traditional breathing detection approaches involving intrusive devices are uncomfortable for long-term continuous monitoring. While contactless detection approaches utilizing radio-frequency (RF) signals or acoustic signals mainly focus on sensing the changes of chest and abdomen displacements, which are not a good indicator recording breathing event due to existing false body movements. In this article, we present Wi-Tracker, a contactless breathing detection system based on commercial off-the-shelf (COTS) smartphones, which detects breathing event through capturing the Doppler effect caused by human exhaled airflow on the reflected acoustic wave. Specifically, Wi-Tracker uses the speaker on smartphone to transmit ultrasound signals and its microphone to receive the reflected acoustic signals recording breathing event. Then, we adopt a cumulative power spectral density (CPSD) method to extract fine-grained breathing pattern from the received signals. Finally, we design algorithms to accurately capture the breathing event from the extracted breathing pattern. We evaluate Wi-Tracker with six volunteers for a period of one month. Experimental results show that Wi-Tracker is able to achieve contactless breathing detection with a mean estimation error (MEE) of 0.17 bpm, which is even better as compared to RFID-based or WiFi-based approaches.

Index Terms—Acoustic sensing, breathing airflow detection, contactless detection, Doppler effect, smartphone.

I. INTRODUCTION

IT IS a well-known fact that the breathing rate of human is an important indicator revealing an individual's health condition. Therefore, it is critical to achieve accurate and continuous breathing detection for early treatment and warning of

Manuscript received 8 May 2022; revised 16 August 2022 and 27 October 2022; accepted 10 November 2022. Date of publication 15 November 2022; date of current version 6 February 2023. This work was supported in part by the National Natural Science Foundation of China under Grant 62202001 and Grant 61972081; in part by the Natural Science Foundation of Shanghai under Grant 22ZR1400200; in part by the Innovation Support Program for Returned Overseas Students in Anhui Province under Grant 2021LCX032; in part by the Key Research and Development Project of Anhui Province under Grant 2022O07020001; and in part by the Science Research Foundation of Anhui University of Finance and Economics under Grant ACKYC22091. This article was presented in part at the 16th International Conference on Wireless Algorithms, Systems, and Applications (WASA), Nanjing, China, June 25–27, 2021 [DOI: 10.1007/978-3-030-85928-2_4]. (Corresponding author: Shan Chang.)

Wei Liu, Feng Li, and Yong Xu are with the School of Management Science and Engineering, Anhui University of Finance and Economics, Bengbu 233030, China (e-mail: liuwei628@ufe.edu.cn).

Shan Chang, Shizong Yan, and Ye Liu are with the School of Computer Science and Technology, Donghua University, Shanghai 201620, China (e-mail: changshan@dhu.edu.cn).

Digital Object Identifier 10.1109/JIOT.2022.3222202

several respiratory diseases. Initially, the researchers use some special sensing devices, including capnometer [2] and pulse oximeter [3] to collect the useful data (e.g., ECG signals [4]) which record human vital signs. Although these methods have achieved high accuracy in breathing monitoring, there are invasive and uncomfortable for the patients. The reason is they usually require users to wear many different sensors during the test. In order to overcome the limitation, it is highly desirable to build a contactless breathing monitoring system without requiring users to wear any sensors.

Recently, there is a new trend of using the data collected by camera [5], [6], [7], [8], [9], [10], [11], Radar (e.g., Doppler radar, ultra wideband (UWB) radar, frequency-modulated continuous wave (FMCW) radar, and millimeter-Wave (mmWave) radar) [12], [13], [14], [15], [16], [17], [18], [19], [20], customized audio devices [21], RFID readers/tags [22], [23], [24], [25], [26], [27], [28], [29], [30], WiFi devices [31], [32], [33], [34], [35], [36], [37], [38], [39], [40], [41], or built-in acoustic devices on smartphone [42], [43], [44] to achieve contactless vital signs detection. However, vision-based approaches usually require a relatively good condition of environment light, and raise privacy concerns due to existing sensitive image data. Deploying dedicated or customized hardware devices incur high cost and low flexible, which prevent them for long-term and large-scale deployment and implementation. More importantly, however, most of the existing works used to detect breathing event are focusing on an indicator called chest and abdomen displacements. In other words, they achieve contactless breathing monitoring by sensing the displacement of human chest and abdomen utilizing wireless or acoustic signals. However, chest and abdomen displacements are not a good indicator recording breathing event once user's chest and abdomen are covered by thick obstacles. In particular, for people suffering from obstructive sleep apnea (OSA), their chests and abdomens could still keep moving as if they are breathing normally while they are going into respiratory arrest [21].

In order to overcome the above limitations, we further consider whether it is feasible to achieve contactless breathing monitoring by utilizing acoustic signals generated by the build-in acoustic devices on smartphone to sense the change of exhaled airflow rather than chest and abdomen displacements. Theoretically, the existing commercial off-the-shelf (COTS) smartphones can be transformed into an active sonar system. That is, the speaker on smartphone can be programmed to transmit ultrasound signals and its microphone can be used to receive the reflected acoustic signals simultaneously. Therefore, the breathing event could be detected by

extracting the Doppler effect caused by human exhaled airflow on the reflected acoustic wave. However, there exist two key challenges need to be solved in order to build a contactless breathing airflow detection system on smartphone. First, the intensity of the exhaled airflow from breathing is really weak, it is challenging to extract fine-grained breathing pattern recording the change of breathing event from the reflected acoustic signals. Second, people may move their bodies when they breathe naturally, it is challenging to remove irrelevant event recording the body movement from the reflected acoustic signals.

To solve the above challenges, we first study the feasibility of utilizing the acoustic signals generated by build-in acoustic devices on smartphone to sense the change of human exhaled airflow rather than chest and abdomen displacements, and find that the PSD of the received acoustic signals can be used to record the Doppler effect caused by human exhaled airflow on the reflected acoustic wave. Then, we design an effective algorithm called cumulative power spectral density (CPSD)-based peak detection, which accumulates all PSD value along the given frequency band, to eliminate frequency interference to extract fine-grained breathing pattern from the received acoustic signals. Finally, we observe that the characteristic of Doppler effect caused by human body movement is different compared to the exhaled airflow caused, and design an algorithm called fake peak removal to further remove irrelevant event from the received acoustic signals. Based on the above research, Wi-Tracker can achieve accurate and reliable contactless breathing detection.

Contributions: Wi-Tracker makes the following main contributions.

- 1) We take a new step toward achieving contactless breathing detection by utilizing acoustic signals generated by the build-in acoustic devices on smartphone to sense the change of human exhaled airflow.
- 2) We design an algorithm called CPSD-based peak detection to extract fine-grained breathing pattern which records the Doppler effect caused by human exhaled airflow on the reflected acoustic wave.
- 3) We design an algorithm called fake peak removal to eliminate body movement interference existed in the reflected acoustic signals to further improve the detection accuracy of our Wi-Tracker.
- 4) We deploy Wi-Tracker with a COTS smartphone and conduct extensive experiments with six volunteers (four adults and two children) for a period of one month. The experimental results demonstrate that with acoustic signals alone, Wi-Tracker is able to achieve about 0.17 bpm mean estimation error (MEE) for breathing detection, which is even better as compared to RFID-based or WiFi-based approaches.

The remainder of this article is organized as follows. Section II briefly summarizes related literature. Section III introduces the preliminaries. In Section IV, we present our system design. The evaluation results are presented in Section V. Section VI further discusses the limitations and opportunities of our Wi-Tracker. We conclude this article in Section VII.

II. RELATED WORK

In general, the existing vital signs detection systems can be widely classified as contact-based and contactless-based (i.e., based on RF or acoustic signals) approaches. In this section, we briefly review these works and compare them with Wi-Tracker.

A. Contact-Based Approaches

The traditional vital signs detection systems require user to wear dedicated sensor devices (e.g., capnometer [2] or pulse oximeter [3]). However, deploying dedicated devices incur high cost and low flexible. In order to overcome the limitation, some recent works of breathing monitoring adopt wearable smartwatch with motion sensors to collect data recorded human breathing information [45], [46], [47], [48], [49], [50], [51]. Although these approaches can achieve low cost and high accuracy, they are invasive and uncomfortable for continuous monitoring, especially for some special social groups, including children, elderly, and disabled people.

B. RF-Based Approaches

Recently, most of the contactless vital signs monitoring systems are the RF signals-based detection mechanisms, which leverage various signals generated by Doppler radar, UWB radar, FMCW radar, mmWave radar [12], [13], [14], [15], [16], [17], [18], [19], [20], RFID readers/tags [22], [23], [24], [25], [26], [27], [28], [29], [30], and WiFi devices [31], [32], [33], [34], [35], [36], [37], [38], [39], [40], [41] to detect one's chest and abdomen displacements during breathing. Although these works can achieve high accuracy without wearing any sensors, they usually require customized hardware with large bandwidth and high frequency, and thus incur low flexible and high cost, which greatly limit their applications in practice. Particularly, chest and abdomen displacements are not a good indicator recording breathing event due to existing false body movements. For instance, it is difficult to detect one's chest and abdomen displacements using current approaches when their chests and abdomens are covered by thick quilt or blanket during breathing. And the users suffering OSA could stop breathing (i.e., only inhaled airflow existed) but their chests and abdomens may still move as if the users were breathing normally.

C. Acoustic-Based Approaches

Most related to this article is the acoustic-based approaches, such as the use of customized audio devices or built-in audio devices of smartphone for sensing the vital signs of breathing rate. Wang et al. [21] used acoustic signals transmitted by customized speaker and microphone to detect ones breathing rate. Therefore, their solution requires additional hardware infrastructure, which is expensive and impractical. In order to overcome the limitation of the above-mentioned approaches, Nandakumar et al. [42] first achieved a novel contactless breathing monitoring system by transforming the smartphone into an active sonar system that emits frequency-modulated sound signals and listens to their reflections. After

that, Xu et al. [43] designed BreathListener, which leverages acoustic devices on smartphone to obtain the fine-grained breathing waveform for drivers in real driving environments. Wang et al. [44] presented SonarBeat, which leverages a phase-based active sonar to monitor breathing rate with smartphone. Although these works [42], [43], [44] can achieve satisfactory performance of breathing monitoring by directly utilizing built-in audio devices of smartphone, they also capture breathing event by detecting the displacements of human chest and abdomen.

In order to overcome the above limitations, we should build an ideal breathing monitoring system that 1) is completely contactless and nonintrusive; 2) incurs low cost; 3) leverages the existing COTS devices (i.e., smartphone); and 4) directly senses exhaled airflow from one's breathing rather than chest and abdomen displacements.

III. PRELIMINARIES

In this section, we first briefly introduce the theoretical model of Doppler effect caused by human exhaled airflow. Then, we conduct a preliminary experiment for verifying the feasibility of the theoretical model.

A. Acoustic Doppler Effect Analysis

Theoretically, the basic idea of achieving contactless breathing monitoring utilizing acoustic signals is the exhaled airflow of human can be seen as a turbulence so that the acoustic wave could be scattered by the exhaled airflow [21]. Briefly, the turbulence from the exhaled airflow mainly contains two parts, including regular and irregular airflow. Thus, the velocity of the turbulence at time t can be denoted as

$$v_t = \bar{v}_t + \tilde{v}_t \quad (1)$$

where \bar{v}_t represents the main velocity of exhaled airflow, which is contributed by the regular airflow having relatively steady norm and direction, and \tilde{v}_t represents the secondary velocity of exhaled airflow, which is contributed by the irregular airflow whose norm and direction change with time. If we project v_t to the line between the sensing device and the scatterer [21], the projection result will be denoted as

$$|v_t| \times \cos(\gamma_t) = |\bar{v}_t| \times \cos(\alpha_t) + |\tilde{v}_t| \times \cos(\beta_t). \quad (2)$$

γ_t , α_t , and β_t are the angle of v_t , \bar{v}_t , and \tilde{v}_t , respectively. Considering the traditional formula computing Doppler shift is given by

$$\Delta f = \left(\frac{\pm 2V}{C} \right) \times f. \quad (3)$$

Thus, we can further derive the Doppler frequency shift [21] caused by the exhaled airflow on the reflected acoustic wave as

$$\Delta f = \pm 2f \times \frac{|\bar{v}_t| \times \cos(\alpha_t) + |\tilde{v}_t| \times \cos(\beta_t)}{C} \quad (4)$$

where C is a constant denoting the speed of sound. It can be seen that the almost symmetric frequency shifts Δf around f will appear if the angle α_t is set to around $\pi/2$.

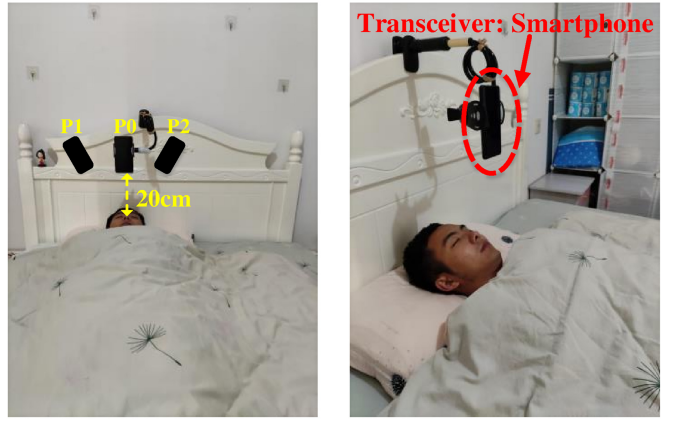


Fig. 1. Practical deployment of Wi-Tracker.

B. Feasibility Verification

In this section, we conduct a preliminary experiment to verify the feasibility of sensing the exhaled airflow utilizing acoustic signals generated by the built-in acoustic devices on smartphone. Specifically, an existing COTS smartphone is transformed into an active sonar system. Then, the speaker on smartphone is programmed to transmit continuous ultrasound signals at the frequency of 20 kHz, which is inaudible to the human ear. Meanwhile, the microphone on smartphone is utilized to receive the reflected acoustic signals with the sampling rate of 48 kHz. Note that the reflected acoustic wave will be scattered by the exhaled airflow of human when the people breathe out carbon dioxide. The system deployment of Wi-Tracker is shown in Fig. 1. We first place the smartphone (i.e., XIAOMI MIX2) at position P0 and set the sensing distance between user's face and the bottom of smartphone to 20 cm. The speaker on smartphone points toward the effective sensing area passing human exhaled airflow. Then, the volunteer is asked to keep breathing 30 s naturally first without wearing a face mask. After that, the volunteer is asked to keep breathing 30 s with wearing a face mask.

The experimental results are shown in Fig. 2. There appear some periodic micro-Doppler frequency shifts (about 200 Hz) whose rhythm are corresponding to each breathing event when user breathes naturally without wearing a face mask, as shown in Fig. 2(a). However, we can observe in Fig. 2(b) that the periodic micro-Doppler frequency shift disappears when user wears a face mask during breathing. The experimental results demonstrate that it is feasible to sense Doppler effect caused by human exhaled airflow on the reflected acoustic wave to achieve contactless breathing detection by utilizing acoustic signals generated by the built-in acoustic devices on smartphone.

IV. SYSTEM DESIGN

In this section, we introduce the system design of Wi-Tracker, including system overview, data processing, and breathing detection. Note that the module of data collection has been introduced briefly in Section III-B.

Algorithm 1 CPSD-Based Peak Detection

Input: Given a segment of PSD signals: $PSD_{\{[t_1, t_e], [f_1, f_E]\}} = \{PSD_{(t_1, f_1)}, \dots, PSD_{(t_1, f_E)}, \dots, PSD_{(t_e, f_1)}, \dots, PSD_{(t_e, f_E)}\}$;

Output: Local peak set: $LocalPeakSet$;

- 1: $AccuPSD, FilterPSD, NormPSD \leftarrow \emptyset, \emptyset, \emptyset$;
- 2: $LocalPeakSet \leftarrow \emptyset$;
- 3: **for** $i = 1:E$ **do**
- 4: $sumPSD_{t_i} \leftarrow 0$;
- 5: **for** $j = 1:E$ **do**
- 6: $sumPSD_{t_i} \leftarrow sumPSD_{t_i} + PSD_{(t_i, f_j)}$;
- 7: **end for**
- 8: Add $sumPSD_{t_i}$ into $AccuPSD_{t_i}$;
- 9: **end for**
- 10: $FilterPSD \leftarrow Filter(AccuPSD, len)$;
- 11: $NormPSD \leftarrow Normalize(FilterPSD)$;
- 12: $Pheight \leftarrow \alpha * Mean(NormPSD)$;
- 13: $MaxSet \leftarrow FindLocalMaxs(NormPSD)$; /* $MaxSet = \{m_k, 1 \leq k \leq K\}$ */
- 14: **for** $k = 1:K$ **do**
- 15: **if** $amplitude(m_k) > Pheight$ **then**
- 16: add m_k into $LocalPeakSet$;
- 17: **end if**
- 18: **end for**
- 19: **Return** $LocalPeakSet$.

A. System Overview

The basic idea of Wi-Tracker is to detect breathing event through capturing the Doppler effect caused by the exhaled airflow on the reflected acoustic wave. As shown in Fig. 3, Wi-Tracker is composed of three modules that operate in a sequential manner.

1) *Data Collection*: The speaker on smartphone is programmed to transmit sinusoidal sound wave at 20 kHz, and the reflected acoustic signals recording the change of exhaled airflow are collected by utilizing the microphone on smartphone with sampling rate of 48 kHz.

2) *Data Processing*: Considering the raw audio data received by the microphone contains ambient noises imposed by the environment, Wi-Tracker first filters out the noise by applying a high-pass filter. Then, Wi-Tracker computes the PSD of filtered acoustic signals to obtain the micro-Doppler frequency shift caused by human exhaled airflow. Finally, a new method called CPSD is used to extract fine-grained breathing pattern from the filtered acoustic signals.

3) *Breathing Detection*: After obtaining the fine-grained breathing pattern, Wi-Tracker first designs a CPSD-based peak detection algorithm to capture the possible breathing event from the pattern. Then, an algorithm called fake peak removal is designed to further remove the peaks caused by human body movement to achieve accurate breathing detection.

B. Data Processing

1) *High-Pass Filtering and PSD Computing*: It is inevitable that the raw acoustic signals receiving by the microphone on smartphone contain ambient noise which could originate from the environment-related changes, including talking, whistling, playing, etc. As shown in Fig. 4(a), we can clearly observe that there exist an ambient noise existed

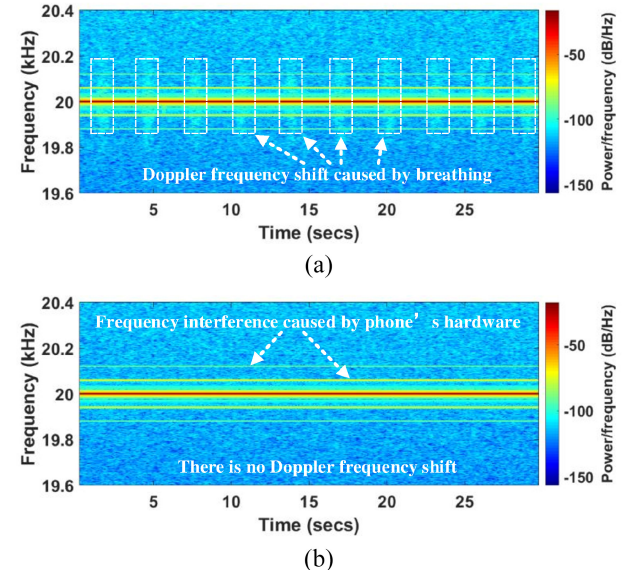


Fig. 2. Variation of Doppler frequency shift under different breathing conditions. (a) Breathing without wearing a face mask. (b) Breathing with wearing a face mask.

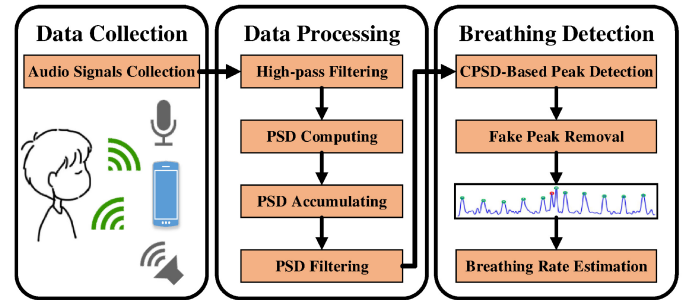


Fig. 3. System architecture of Wi-Tracker.

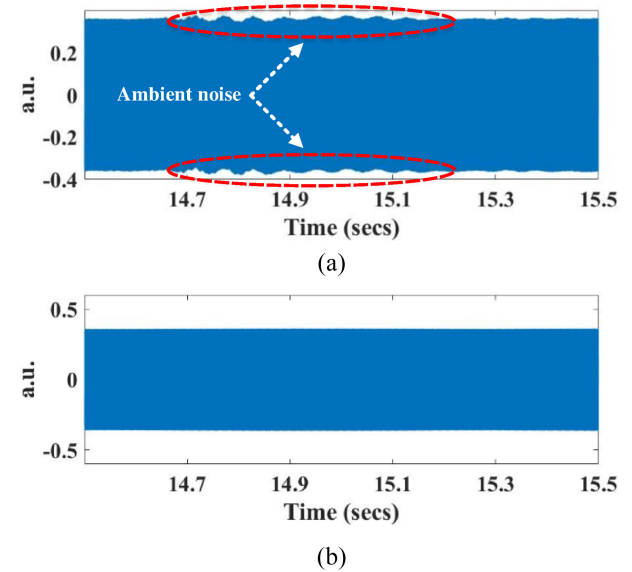


Fig. 4. Processed acoustic signals. (a) Received original acoustic signals. (b) Acoustic signals after applying high-pass filter.

in the received acoustic signals, and its frequencies is about 20 Hz. Considering the fact that the highest frequency of ambient noises is far below 18 kHz and the actual Doppler

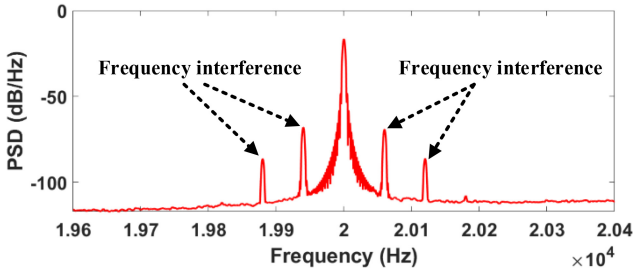


Fig. 5. Accumulated PSD value of the frequency points.

frequency shift caused by the exhaled airflow of human is below 200 Hz [21], we thus apply a high-pass filter to remove the ambient noises with frequency below 18 kHz. The filtering results are shown in Fig. 4(b). It can be seen that the ambient noise existed in the raw acoustic signals is filtered out after applying a high-pass filter. Then, the filtered acoustic signals are transformed into time–frequency domain signals recording the change of Doppler frequency shift by using the short-time Fourier transform (STFT) method. Specifically, the PSD of filtered acoustic signals can be calculated by

$$\text{PSD}_{R(t)} = \frac{\text{STFT}_N(R(t))^2}{N} \quad (5)$$

$$R(t) = \sum_{i \in \Omega} A_i \sin(2\pi f t + \varphi_i) \quad (6)$$

where f and t are the frequency and time of received acoustic signals $R(t)$, respectively. A_i denotes a coefficient representing the amplitude attenuation of acoustic signal in path i , φ_i denotes the phase change corresponding to the initial phase φ during the propagation in path i , Ω is the set of all propagation paths of transmission signal, and N is the points used discrete Fourier transform (DFT) [43].

As shown in Fig. 2(a), we can clearly observe that the PSD of echo signal shows some periodic micro-Doppler frequency shifts whose rhythm are corresponding to each breathing event, which implies that the breathing event can be detected by extracting the Doppler effect caused by the exhaled airflow on the reflected acoustic wave. Note that the main frequency of the received acoustic signal is always kept at a frequency of 20 kHz, the reason is the main component of echo signal is the reflected ultrasound signal. In addition, it can be seen from Figs. 2(b) and 5 that there are some interference frequency points which have a higher PSD value than exhaled airflow caused. We speculate the reason is the echo signal could be disturbed due to complex layout of hardware on smartphone. Considering the range of Doppler frequency shift caused by human exhaled airflow on the reflected acoustic wave is lower than 200 Hz, we only select the PSD within the frequency band [19.6 kHz, 20.4 kHz] to obtain the Doppler frequency shift recording breathing event.

2) *PSD Accumulating and Filtering*: As shown in Fig. 2, we can conclude that the PSDs of interference frequency points have a relatively stable value over time. Based on this observation, a method called CPSD is used to eliminate frequency interference so that the coarse-grained

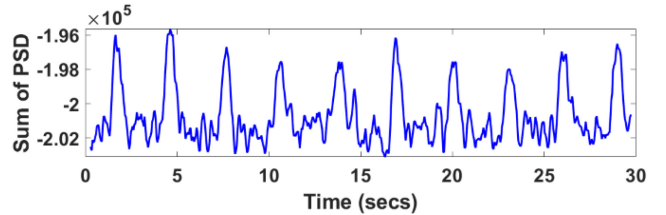


Fig. 6. Accumulated PSD signals.

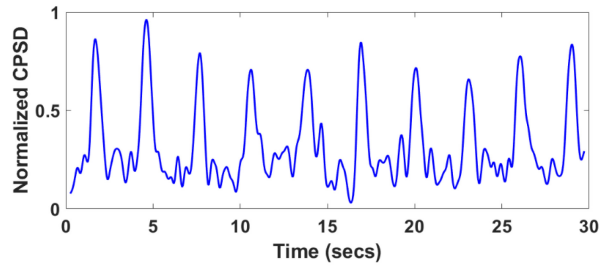


Fig. 7. Processed PSD signals.

human breathing pattern could be extracted. Specifically, Wi-Tracker first accumulates all power spectral density along the frequency band from 19.6 to 20.4 kHz in the spectrogram as shown in Fig. 2(a). The accumulated results are shown in Fig. 6. It can be seen that the ten breathing events shown in Fig. 2(a) have been extracted roughly (i.e., one peak is corresponding to one breathing event). Although the frequency interference can be eliminated after applying the method, the accumulated PSD signals still contain some noises. Then, a moving average filter with a Gaussian window is applied to further remove the noises existed in the accumulated PSD signals so that the fine-grained breathing pattern recording the change of exhaled airflow of human can be obtained. Finally, the filtered PSD signals are normalized between 0 and 1 for performing breathing detection. The processed PSD signals are shown in Fig. 7. We can clearly observe that the processed PSD signals are neater and smoother than before, and all ten breathing events can be observed.

C. Breathing Detection

1) *CPSD-Based Peak Detection*: From Fig. 7, we observe the amplitude changes of processed PSD signals present some periodic ripple-like patterns whose rhythm are corresponding to each breathing event. This observation reveals that the breathing event will be detected as long as the peaks recording the change of exhaled airflow can be accurately captured. Furthermore, the human breathing rate can be obtained by calculating peak-to-peak intervals of the captured peaks. To achieve this goal, an algorithm called CPSD-based peak detection is designed, described as Algorithm 1. Specifically, as described in lines 1–9 of Algorithm 1, Wi-Tracker first adopts a cumulative PSD method which accumulates all power spectral density along the given frequency band [f_1 kHz, f_2 kHz] to extract coarse-grained human breathing pattern. After that, as shown in line 10 and line 11 of Algorithm 1, Wi-Tracker applies a moving average filter to further remove

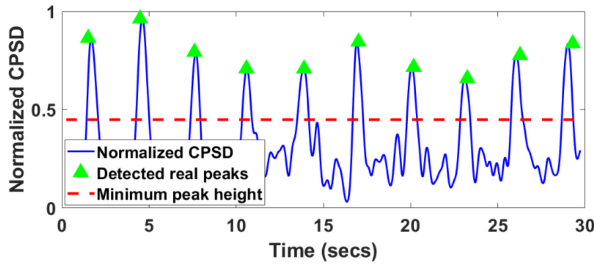


Fig. 8. Result of peak detection after applying Algorithm 1.

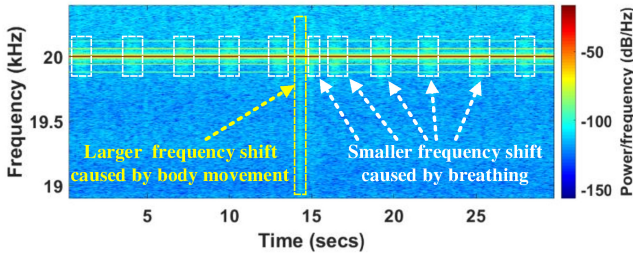


Fig. 9. Doppler frequency shift under different activities.

Algorithm 2 Fake Peak Removal

Input: Local peak set: $LocalPeakSet = \{p_k, 1 \leq k \leq K\}$; PSD signals of lower frequency band: $PSD_{([t_1, t_e], [f_{S'}, f_{E'}])} = \{PSD_{(t_1, f_{S'})}, \dots, PSD_{(t_1, f_{E'})}, \dots, PSD_{(t_e, f_{S'})}, \dots, PSD_{(t_e, f_{E'})}\}$;

Output: Real peak set: $RealPeakSet$;

```

1:  $T_{sum} \leftarrow \delta$ ;
2: for  $k = 1:K$  do
3:    $loc \leftarrow location(p_k)$ ;
4:    $sumPSD_{t_{loc}} \leftarrow 0$ ;
5:   for  $j = S':E'$  do
6:      $sumPSD_{t_{loc}} \leftarrow sumPSD_{t_{loc}} + PSD_{(t_{loc}, f_j)}$ ;
7:   end for
8:   if  $sumPSD_{t_{loc}} < T_{sum}$  then
9:     add  $p_k$  into  $RealPeakSet$ ;
10:  end if
11: end for
12: Return  $RealPeakSet$ .

```

noise interference and normalizes filtered signals to obtain fine-grained human breathing pattern. Then, a minimum peak height is set to differentiate between the peaks caused by human exhaled airflow and the others, as shown in line 12 of Algorithm 1. Finally, Wi-Tracker uses a classical peak finding algorithm to capture the real peaks recording the breathing events from the processed PSD signals, as shown in lines 13–19 of Algorithm 1. In our experiment, we find a short Gaussian window with length of 10 is good enough to remove the noises and empirically set α , f_1 , and f_E as 1.4, 19.6, and 20.4, respectively. The results of peak detection applying Algorithm 1 are shown in Fig. 8. It can be seen that the minimum peak height we calculated is effective and all the peaks recording the breathing events can be detected accurately.

2) *Fake Peak Removal and Breathing Rate Estimation*: Although the breathing event can be detected by capturing the peaks recording the change of exhaled airflow, we have to consider a situation where some body movements exist inevitably when people breathe naturally. To observe the influence of human body movement on the reflected acoustic wave, the

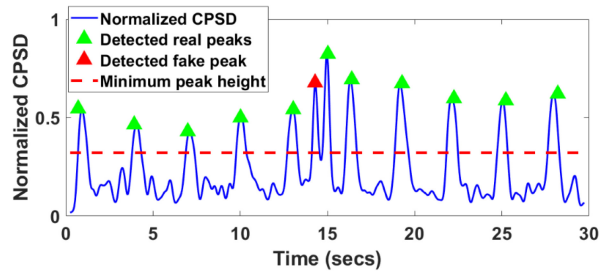


Fig. 10. Result of fake peak removal after applying Algorithm 2.

volunteers are asked to move their body one time randomly when they keep breathing naturally. The experiment result is shown in Fig. 9. It can be seen that there is a larger Doppler frequency shift body movement caused compared with human exhaled airflow. Based on this observation, we should further remove the fake peak recording the human body movement from the peaks captured by applying Algorithm 1. To achieve the goal, an algorithm called fake peak removal is designed to remove the fake peak to enhance the robustness of our Wi-Tracker, described as Algorithm 2. Specifically, as described in lines 1–7 of Algorithm 2, for each local peak captured by applying Algorithm 1, Wi-Tracker accumulates all PSD value along a lower frequency band $[f_{S'} \text{ kHz}, f_E \text{ kHz}]$ again. Then, the accumulated PSD value is used to be compared with δ a threshold used to differentiate the peaks caused by human body movement or their exhaled airflow. Finally, Wi-Tracker only retains the peaks recording the breathing events rather than human body movement, as shown in lines 8–12 of Algorithm 2. In our experiment, we observe that a relatively lower frequency band $[f_{S'}=19 \text{ kHz}, f_E=19.5 \text{ kHz}]$ and threshold $\delta = -1.3 * 10^5$ are good enough to remove the fake peak recording the human body movement. The result of fake peak removal applying Algorithm 2 is shown in Fig. 10. It can be seen that the real peaks recording the breathing events are also detected accurately and the fake peak recording the human body movement shown in Fig. 9 is removed successfully. Once the real peaks are detected by the algorithms, the human breathing rate R^E can be estimated by using the following equation:

$$R^E = \frac{N}{T_E - T_S} * 60 \quad (7)$$

where T_S and T_E are the start time (in seconds) and end time of the given PSD signals, and N is a total number of peaks detected by the algorithms.

V. EVALUATION

In this section, we conduct extensive experiments to evaluate the performance of our Wi-Tracker. First, we introduce the system implementation and experiment settings. Then, the overall performance of Wi-Tracker is evaluated and compared with the state-of-the-art methods, including RF-based and WiFi-based. Finally, the robustness of Wi-Tracker is further evaluated by considering various factors.

A. Implementation

1) *System Implementation*: As shown in Fig. 1, our system is implemented by utilizing existing COTS smartphones, including XIAOMI MIX2 and GoogleNexus 5X. Specifically, the speaker on smartphone is programmed to transmit ultrasound signals at the frequency of 20 kHz, which is inaudible to human ear. We use the microphone on smartphone to receive reflection waves at the sampling rate of 48 kHz. Then, a laptop with 8-GB memory and 1.8-GHz CPU is used to process collected data, and the proposed algorithms are programmed in MATLAB R2018b to detect breathing event.

2) *Experiment Settings*: We evaluated Wi-Tracker with six volunteers, including four adults (i.e., three males and one female) and two children (i.e., one boy and one girl) and collected one month of breathing data in total. Their ages are in the range of 9–30 years, with the weight from 23 to 70 kg. During the experiment, each of the volunteer is asked to test for 20 min per day, and the ground truth of breathing rate is obtained by using NEULOG Respiration Monitor Logger Sensor [52]. Note that all experiments involving human behaviors are approved by our IRB.

3) *Performance Metrics*: We first employ one widely used metric in breathing monitoring field called mean estimation error (i.e., MEE) to evaluate system performance. MEE is an absolute difference between the estimated breathing rate and actual breathing rate. The unit used to calculate breathing rate is breath per minute (i.e., bpm). Specifically

$$\text{MEE} = \frac{\sum_{i=1}^k |R_k^E - R_k^A|}{k} \quad (8)$$

where R_k^A and R_k^E correspond to the actual and estimated breathing rate, respectively.

In addition, considering apnea event is an important indicator recording human health condition, we then define a novel metric called detection accuracy of apnea (i.e., DAA) to further evaluate the performance of Wi-Tracker. Specifically

$$\text{DAA} = \frac{\sum_{i=1}^n \left(1 - \frac{|T_n^E - T_n^A|}{T_n^A}\right)}{n} * 100\% \quad (9)$$

where T_n^A and T_n^E correspond to the actual and estimated duration of apnea event, respectively. Specifically

$$T_n^A = T_{e_n}^A - T_{s_n}^A \quad (10)$$

where $T_{e_n}^A$ and $T_{s_n}^A$ are the end time and start time of the n th apnea event detected by the ground truth (i.e., NEULOG Respiration Monitor Logger Sensor). And

$$T_n^E = T_{e_n}^E - T_{s_n}^E \quad (11)$$

where $T_{e_n}^E$ and $T_{s_n}^E$ are the end time and start time of the n th apnea event estimated by our Wi-Tracker.

B. Overall Performance

In the overall evaluation, we first evaluate the performance of Wi-Tracker for different users. Then, we compare our approach with the state-of-the-art breathing detection systems.

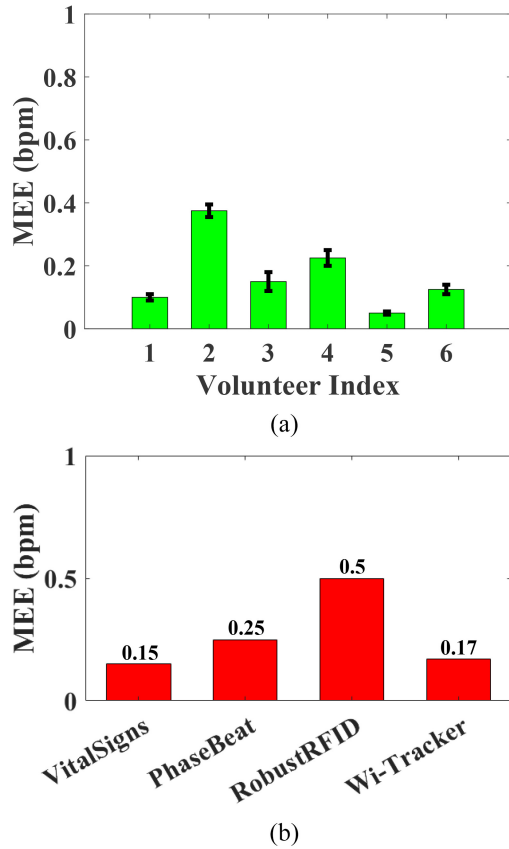


Fig. 11. Overall performance. (a) Performance of Wi-Tracker. (b) Wi-Tracker versus other systems.

1) *Evaluation of Breathing Event Detection*: Fig. 11(a) illustrates the breathing event detection performance of Wi-Tracker in terms of MEE for each individual volunteer. As we can see, the MEE of most volunteers is below 0.2 bpm with a small standard deviation shown in the black error bar, and the MEE of all volunteers is around 0.17 bpm. Note that the performance of volunteers 2 and 4 is slightly lower (i.e., higher than 0.2 bpm) than others. The reason is that these two volunteers are children exhaled slightly weaker airflow during sleep compared with other adults, which would cause the misdetection because of the weaker airflow causing smaller Doppler frequency shift. Overall speaking, our Wi-Tracker can achieve satisfactory performance for breathing monitoring.

2) *In Comparison to the State-of-the-Art Systems*: We further compare our Wi-Tracker with other three state-of-the-art contactless breathing detection systems, including WiFi-based systems called VitalSigns [33] and PhaseBeat [34], and RFID-based system called RobustRFID [24]. The performance of breathing rate estimation reported in each system is shown in Fig. 11(b). As we can see that the other three detection systems have MEE of 0.15, 0.25, and 0.5 bpm for breathing monitoring, respectively. Specifically, our Wi-Tracker outperforms RobustRFID (i.e., RFID-based system) with an average 0.33 bpm improvement of breathing monitoring performance, and achieves comparable performance without deploying additional devices compared with VitalSigns and PhaseBeat (i.e., WiFi-based systems). Note that the other three methods

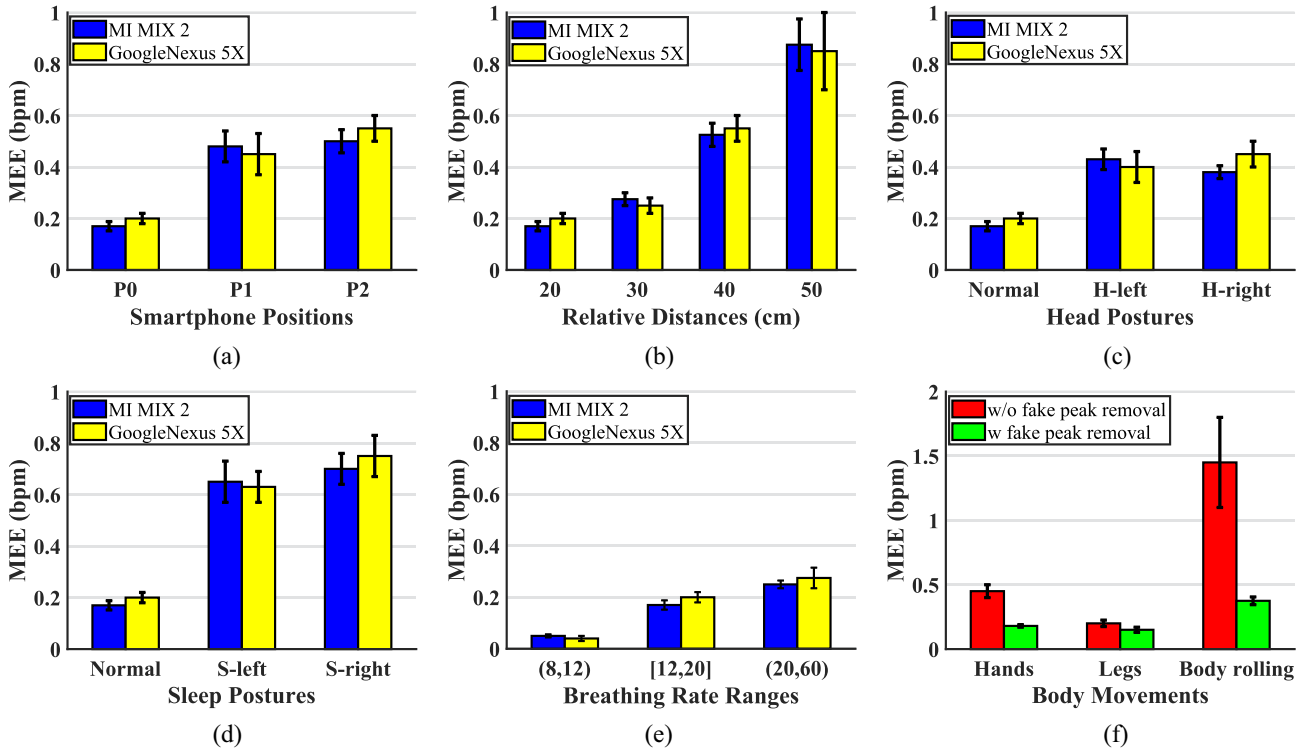


Fig. 12. MEE under different impact factors. (a) Smartphone positions. (b) Relative distances. (c) Head postures. (d) Sleep postures. (e) Breathing rate ranges. (f) Body movements.

achieve contactless breathing monitoring by sensing chest and abdomen displacements, while our Wi-Tracker detects breathing event by sensing human exhaled airflow which is a better indicator of breathing monitoring. In conclusion, Wi-Tracker provides a novel method for contactless breathing monitoring and achieves comparable or even better detection performance as compared to RFID-based or WiFi-based approaches.

C. Impact of Various Factors

In this section, we perform a detailed study to discuss the robustness of Wi-Tracker under various factors, including smartphone positions, relative distances, head postures, sleep postures, breathing rate ranges, body movements, and wind intensity.

1) *Smartphone Positions*: We first place the smartphone at different positions shown in Fig. 1 (i.e., P0, P1, and P2) to study the impact of smartphone positions. Then, we invite two volunteers to test ten times for each position and keep breathing 3 min in each time. In addition, we ask them to simulate apnea event one time randomly during each test. The experimental results are shown in Figs. 12(a) and 13(a). It is observed that the MEE and DAA of system under different smartphone positions are 0.19, 0.47, and 0.53 bpm, and 97.8%, 97%, and 97%, respectively. In general, the system performance is not sensitive to given two different types of COTS smartphones. Particularly, we find Wi-Tracker has a slightly lower MEE than other positions when the smartphone is placed at position P0. The reason is when the smartphone is tilted to one side, the effective sensing area passing the exhaled airflow becomes smaller so that the useful signals recording

Doppler frequency shift are much weaker. Note that the DAAs are relatively stable in the experiment. The reason is the apnea events usually occur less frequently (i.e., 20 times) and have a longer duration (i.e., usually more than 10 s) so that it is relatively easy to detect apnea events accurately. Overall speaking, Wi-Tracker can achieve satisfactory performance for breathing monitoring as long as the speaker on smartphone points toward human exhaled airflow directly.

2) *Relative Distances*: We first place the smartphone at position P0 and then adjust the distance between user's head and sensing device ranging from 20 to 50 cm with an interval of 10 cm to study the impact of relative distances. Then, we also invite two volunteers to test ten times for each sensing distance and keep breathing 3 min in each time. Similarly, they also simulate apnea event one time randomly during each test. Figs. 12(b) and 13(b) show the performance of Wi-Tracker under different sensing distance settings. We observe that the MEE and DAA of system under different sensing distances are 0.19, 0.26, 0.54, and 0.86 bpm, and 97.8%, 98.1%, 89.4%, and 74%, respectively. It is clear that the performance of Wi-Tracker degrades obviously when the sensing distance is increased. The reason is the power of the speaker on smartphone is significantly lower than the dedicated acoustic equipment so that the signal strength of received acoustic signals is decreased significantly with increasing sensing distance. Overall speaking, Wi-Tracker can maintain good sensing ability for breathing monitoring within a sensing distance of 40 cm.

3) *Head Postures*: Considering the fact that people may rotate their head to the side when they breathe naturally during

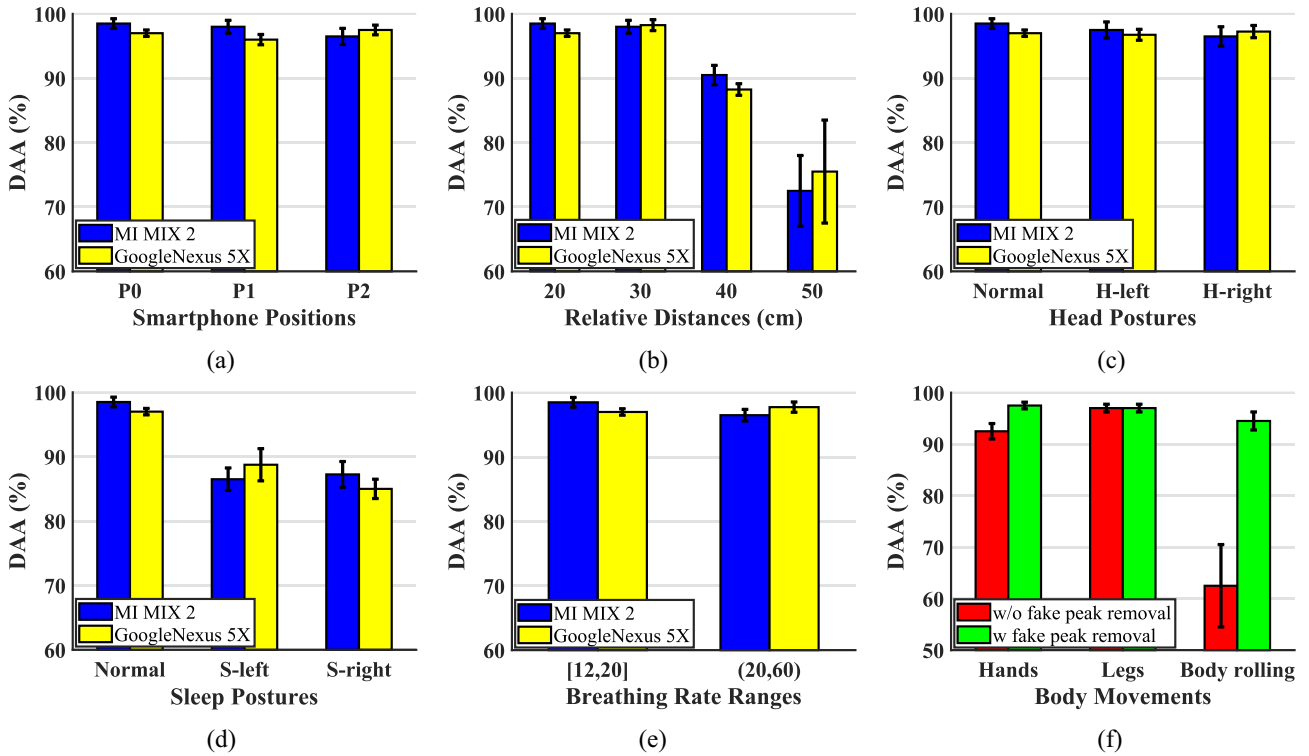


Fig. 13. DAA under different impact factors. (a) Smartphone positions. (b) Relative distances. (c) Head postures. (d) Sleep postures. (e) Breathing rate ranges. (f) Body movements.

sleep, we need to study the impact of head postures for breathing monitoring. For each head posture test, the smartphone is placed at position P0 and the relative distance is set to 20 cm. Figs. 12(c) and 13(c) show the performance of Wi-Tracker for different head postures. “H-left” and “H-right” shown in the figure represent turning their head to the left and right, respectively. We can observe the MEE and DAA of system for different head postures are 0.19, 0.42, and 0.43 bpm, and 97.8%, 97.1%, and 96.9%, respectively. It can be seen that the performance of Wi-Tracker degrades a little when people turn their head to the left or right. The reason is the effective sensing area passing human exhaled airflow becomes smaller so that the weaker acoustic signal recording breathing event could be captured by the receiver. In general, our system is not sensitive enough to the change of head postures and is able to provide robust performance for breathing monitoring.

4) *Sleep Postures:* Considering the fact that people may change their sleep postures (i.e., turning from supine to side) during sleep, we also study the impact of sleep postures for breathing monitoring. In this experiment, the subjects are asked to turn their body from supine to left and right side (about 90°), respectively. And, the speaker of smartphone transmits acoustic wave toward the subject’s side face, the relative distance between subject’s face and smartphone is about 20 cm. Figs. 12(d) and 13(d) show the performance of Wi-Tracker for different sleep postures. Similarly, “S-left” and “S-right” shown in the figure represent turning their body from supine to left and right side, respectively. As we can see the MEE and DAA of system for different sleep postures are 0.19, 0.64, and 0.73 bpm, and 97.8%, 87.6%, and

86.1%, respectively. It can be seen that the performance of Wi-Tracker also degrades obviously when the volunteers change their sleep posture from supine to the lateral positions. The reason is only a part of exhaled airflow could be sensed by the microphone on smartphone when they keep their sleep posture on the side. In order to overcome the limitation, we will try to deploy multiple smartphones or dedicated acoustic equipment to enhance sensing ability of Wi-Tracker in the future work.

5) *Breathing Rate Ranges:* The most common breathing rate of human is range from 8 to 60 bpm, including slow breathing (i.e., 8–12 bpm), normal breathing (i.e., 12–20 bpm), and fast breathing (i.e., 20–60 bpm). The reason why we divide the breathing rate into three different ranges is the range of typical breathing rate of different populations is always different. Specifically, the normal breathing rate of adults is 12–20 times per minute while children and infants are 20–60 times per minute. And the breathing rate of patients with heart or lung diseases may be 8–12 times per minute or even lower. Wi-Tracker should able to provide reliable detection performance no matter the subjects are adults, children or even patients. Therefore, we need to evaluate the performance of Wi-Tracker under different breathing rates. For each breathing rate test, we also invite two volunteers to test ten times and keep breathing 3 min in each time. Note that they need to simulate apnea event during the test of normal and fast breathing and do not simulate apnea event when they keep breathing slowly. The reason is apnea event could be submerged when people breathe slowly. Figs. 12(e) and 13(e) show the system performance under different breathing rates. It can be seen from the figures that the MEE and DAA of system under

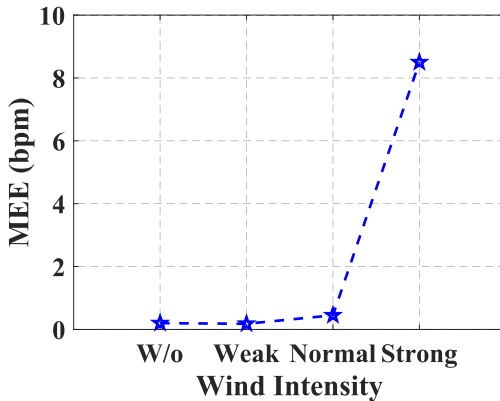


Fig. 14. Breathing detection error as the intensity of interfering airflow varies.

different breathing rates are 0.05, 0.19, and 0.26 bpm, and 97.8% and 97.1%, respectively. It can be seen that although the performance of Wi-Tracker also degrades a little when the breathing rate is increased, it can still achieve satisfactory performance for breathing monitoring no matter the breathing rate is slow, normal, or fast.

6) *Body Movements*: Since body movement generates a larger Doppler frequency shift than their exhaled airflow and further influences the system performance, we need to evaluate the impact of body movements for breathing monitoring. We also invite two volunteers to test ten times under different movement interferences and keep breathing 3 min in each time. They randomly move their limbs or roll whole body several times during the test. Figs. 12(f) and 13(f) show the performance of Wi-Tracker under different body movement interferences. Obviously, the MEE of system is below 0.4 bpm and the average DAA is above 94.5% when the algorithm (i.e., fake peak removal algorithm) is applied. The results demonstrate Wi-Tracker can provide reliable performance under different movement interferences as long as the algorithm we designed is applied.

7) *Wind Intensity*: Our Wi-Tracker works by sensing the human exhaled airflow utilizing acoustic signals generated by build-in acoustic devices on smartphone. If there exists the interfering airflow which also passes the effective sensing area, the performance of Wi-Tracker may degrade severely. To evaluate the impact of the interfering airflow, we conduct a new experiment which utilizes a household air-conditioner to generate interfering airflow toward subject's head. During the experiment, we use a handheld anemometer to measure the airflow speed of the outlet of the air-conditioner. The linear distance between the subject's head and the outlet of the air-conditioner is about 2 m. Then, we adjust the wind intensity of the air-conditioner from weak to strong successively, which includes weak wind (i.e., airflow speed of the outlet is about 0.5 m/s), normal wind (i.e., airflow speed of the outlet is about 2.5 m/s), and strong wind (i.e., airflow speed of the outlet is about 5 m/s). We also invite two volunteers to test system performance under different wind intensities. Fig. 14 shows the breathing detection performance of Wi-Tracker in terms of MEE. As we can see, our Wi-Tracker cannot detect breathing

event accurately when the wind intensity of the air-conditioner is set to strong. The experiment results imply Wi-Tracker is sensitive to strong interfering airflow. Note that people who are sleeping or resting always avoid the strong wind blowing toward their bodies directly.

VI. DISCUSSION

Wi-Tracker takes a new step for achieving contactless breathing detection, which senses human exhaled airflow exploiting built-in acoustic devices on smartphone. Several limitations need to be improved in future work can be summarized as follows.

A. Sensing Distance

As presented in Section V-C, the performance of Wi-Tracker is sensitive to sensing distance between the smartphone and user. The main reason is the transmitting power of speaker on smartphone is limited. Therefore, the microphone on smartphone may not receive sufficiently strong echo signal. In order to overcome the limitation of sensing distance, a potential solution is that we can deploy some dedicated audio devices (i.e., speaker and microphone) or smartphones with high performance for enhancing the transmitting power of the system.

B. Multiposture Scenario

As presented in Section V-C, the performance of Wi-Tracker degrades obviously when the volunteers change their sleep posture from supine to the lateral positions. The main reason is the effective sensing area passing the exhaled airflow cannot be covered completely using only one smartphone. In order to overcome the limitation of sleep posture change, a potential solution is that we can deploy multiple smartphones in multiple locations at the same time for expanding the effective sensing area of the system.

C. Multiuser Scenario

In common with the most existing works, Wi-Tracker can only be applied to detect breathing event when a single person lies on the bed. In other words, Wi-Tracker does not consider the scenario where two or more people lie on the same bed at the same time. Once there are multiple persons lying on the same bed at the same moment, the exhaled airflow exhaled by one person may be interfered by other persons. In order to overcome the limitation of multiuser scenario, a potential solution is that we can use a motor to adjust the direction of the acoustic transceiver for detecting multiple subjects flexibly.

VII. CONCLUSION

In this article, we study the feasibility of using built-in acoustic devices of the smartphone to detect breathing event. In particular, we present a new system called Wi-Tracker for achieving contactless breathing monitoring, which senses human exhaled airflow rather than chest and abdomen displacements by exploiting acoustic signals generated by the COTS smartphones. The proposed method does not require

the people to wear any sensing devices or a camera to record images involving sensitive or private information. We design the algorithms to extract the fine-grained breathing pattern and eliminate body movement interference so that the breathing event can be captured accurately. The experimental results demonstrate that the MEE of Wi-Tracker is around 0.17 bpm for breathing detection and the apnea event can be detected accurately. We believe Wi-Tracker opens up a new way to perform contactless breathing monitoring.

REFERENCES

- [1] W. Liu, S. Chang, S. Yan, H. Zhang, and Y. Liu, "Wi-Tracker: Monitoring breathing airflow with acoustic signals," in *Proc. 16th Int. Conf. Wireless Algorithms Syst. Appl. (WASA)*, 2021, pp. 41–52.
- [2] M. B. Jaffe, "Infrared measurement of carbon dioxide in the human breath: 'Breathe-throug' devices from tyndall to the present day," *Anesthesia Analgesia*, vol. 107, no. 3, pp. 890–904, 2008.
- [3] N. H. Shariati and E. Zahedi, "Comparison of selected parametric models for analysis of the photoplethysmographic signal," in *Proc. Int. Conf. Comput. Commun. Signal Process.*, 2005, pp. 169–172.
- [4] L. Wang, C. Zhao, M. Dong, and K. Ota, "Fetal ECG signal extraction from long-term abdominal recordings based on adaptive QRS removal and joint blind source separation," *IEEE Sensors J.*, vol. 22, no. 21, pp. 20718–20729, Nov. 2022.
- [5] M. Bartula, T. Tigges, and J. Muehlsteff, "Camera-based system for contactless monitoring of respiration," in *Proc. 35th Annu. Int. Conf. IEEE Eng. Med. Biol. Soc. (EMBC)*, 2013, pp. 2672–2675.
- [6] L. A. M. Aarts et al., "Non-contact heart rate monitoring utilizing camera photoplethysmography in the neonatal intensive care unit—A pilot study," *Early Human Develop.*, vol. 89, no. 12, pp. 943–948, 2013.
- [7] K. T. Oh, C. S. Shin, J. Kim, and S. K. Yoo, "Level-set segmentation-based respiratory volume estimation using a depth camera," *IEEE J. Biomed. Health Inform.*, vol. 23, no. 4, pp. 1674–1682, Jul. 2019.
- [8] M. Mateu-Mateus, F. Guedé-Fernandez, M. A. García-González, J. Ramos-Castro, and M. Fernandez-Chimeno, "Non-contact infrared-depth camera-based method for respiratory rhythm measurement while driving," *IEEE Access*, vol. 7, pp. 152522–152532, 2019.
- [9] M. Mateu-Mateus, F. Guedé-Fernandez, M. A. García-González, J. Ramos-Castro, and M. Fernandez-Chimeno, "Camera-based method for respiratory rhythm extraction from a lateral perspective," *IEEE Access*, vol. 8, pp. 154924–154939, 2020.
- [10] C. Coronel et al., "3D camera and pulse oximeter for respiratory events detection," *IEEE J. Biomed. Health Inform.*, vol. 25, no. 1, pp. 181–188, Jan. 2021.
- [11] Y. Wang et al., "Unobtrusive and automatic classification of multiple people's abnormal respiratory patterns in real time using deep neural network and depth camera," *IEEE Internet Things J.*, vol. 7, no. 9, pp. 8559–8571, Sep. 2020.
- [12] Y. S. Lee, P. N. Pathirana, C. L. Steinfort, and T. Caelli, "Monitoring and analysis of respiratory patterns using microwave Doppler radar," *IEEE J. Transl. Eng. Health Med.*, vol. 2, pp. 1–12, 2014.
- [13] F. Adib, H. Mao, Z. Kabelac, D. Katabi, and R. C. Miller, "Smart homes that monitor breathing and heart rate," in *Proc. 33rd ACM Conf. Human Factors Comput. Syst. (ACM CHI)*, 2015, pp. 837–846.
- [14] P. Nguyen, X. Zhang, A. Halbowe, and T. Vu, "Continuous and fine-grained breathing volume monitoring from afar using wireless signals," in *Proc. IEEE Conf. Comput. Commun. (INFOCOM)*, 2016, pp. 1–9.
- [15] C. H. Hsieh, Y. F. Hu Chiu, Y. H. Shen, T.-S. Chu, and Y.-H. Huang, "A UWB radar signal processing platform for real-time human respiratory feature extraction based on four-segment linear waveform model," *IEEE Trans. Biomed. Circuits Syst.*, vol. 10, no. 1, pp. 219–230, Feb. 2016.
- [16] M. Kebe, R. Gadafi, B. Mohammad, M. Sanduleanu, H. Saleh, and M. Al-Qutayri, "Human vital signs detection methods and potential using radars: A review," *Sensors*, vol. 20, no. 5, p. 1454, 2020.
- [17] Z. Yang, P. H. Pathak, Y. Zeng, X. Liran, and P. Mohapatra, "Monitoring vital signs using millimeter wave," in *Proc. 17th ACM Int. Symp. Mobile Ad Hoc Netw. Comput. (MobiHoc)*, 2016, pp. 211–220.
- [18] Z. Yang, P. H. Pathak, Y. Zeng, X. Liran, and P. Mohapatra, "Vital sign and sleep monitoring using millimeter wave," *ACM Trans. Sensor Netw.*, vol. 13, no. 2, pp. 1–32, 2017.
- [19] F. Wang, F. Zhang, C. Wu, B. Wang, and K. J. R. Liu, "ViMo: Multiperson vital sign monitoring using commodity millimeter-wave radio," *IEEE Internet Things J.*, vol. 8, no. 3, pp. 1294–1307, Feb. 2021.
- [20] F. Wang, X. Zeng, C. Wu, B. Wang, and K. J. R. Liu, "Driver vital signs monitoring using millimeter wave radio," *IEEE Internet Things J.*, vol. 9, no. 13, pp. 11283–11298, Jul. 2022.
- [21] T. Wang et al., "Contactless respiration monitoring using ultrasound signal with off-the-shelf audio devices," *IEEE Internet Things J.*, vol. 6, no. 2, pp. 2959–2973, Apr. 2019.
- [22] Y. Yang, J. Cao, and X. Liu, "ER-rhythm: Coupling exercise and respiration rhythm using lightweight COTS RFID," *Proc. ACM Interact. Mobile Wearable Ubiquitous Technol. (ACM UbiComp)*, vol. 3, no. 4, pp. 1–24, 2019.
- [23] L. Chen, J. Xiong, X. Chen, S. I. Lee, D. Zhang, and T. Yan, "LungTrack: Towards contactless and zero dead-zone respiration monitoring with commodity RFIDs," *Proc. ACM Interact. Mobile Wearable Ubiquitous Technol. (ACM UbiComp)*, vol. 3, no. 3, pp. 1–22, 2019.
- [24] Y. Yang, J. Cao, and Y. Wang, "Robust RFID-based respiration monitoring in dynamic environments," *IEEE Trans. Mobile Comput.*, early access, Aug. 24, 2021, doi: [10.1109/TMC.2021.3106954](https://doi.org/10.1109/TMC.2021.3106954).
- [25] C. Yang, X. Wang, and S. Mao, "Respiration monitoring with RFID in driving environments," *IEEE J. Sel. Areas Commun.*, vol. 39, no. 2, pp. 500–512, Feb. 2021.
- [26] X. Liu, J. Yin, Y. Liu, S. Zhang, S. Guo, and K. Wang, "Vital signs monitoring with RFID: Opportunities and challenges," *IEEE Netw.*, vol. 33, no. 4, pp. 126–132, Jul./Aug. 2019.
- [27] Y. Wang and Y. Zheng, "TagBreathe: Monitor breathing with commodity RFID systems," *IEEE Trans. Mobile Comput.*, vol. 19, no. 4, pp. 969–981, Apr. 2020.
- [28] S. Zhang, X. Liu, Y. Liu, B. Ding, S. Guo, and J. Wang, "Accurate respiration monitoring for mobile users with commercial RFID devices," *IEEE J. Sel. Areas Commun.*, vol. 39, no. 2, pp. 513–525, Feb. 2021.
- [29] X. Chang, J. Dai, Z. Zhang, K. Zhu, and G. Xing, "RF-RVM: Continuous respiratory volume monitoring with COTS RFID tags," *IEEE Internet Things J.*, vol. 8, no. 16, pp. 12892–12901, Aug. 2021.
- [30] J. Zhang, J. Yu, Y. Ma, and X. Liang, "RF-RES: Respiration monitoring with COTS RFID tags by Dopplershift," *IEEE Sensors J.*, vol. 21, no. 21, pp. 24844–24854, Nov. 2021.
- [31] W. Liu, S. Chang, Y. Liu, and H. Zhang, "Wi-PSG: Detecting rhythmic movement disorder using COTS WiFi," *IEEE Internet Things J.*, vol. 8, no. 6, pp. 4681–4696, Mar. 2021.
- [32] X. Liu, J. Cao, S. Tang, and J. Wen, "Wi-sleep: Contactless sleep monitoring via WiFi signals," in *Proc. IEEE Real-Time Syst. Symp. (RTSS)*, 2014, pp. 346–355.
- [33] J. Liu, Y. Wang, Y. Chen, J. Yang, X. Chen, and J. Cheng, "Tracking vital signs during sleep leveraging off-the-shelf WiFi," in *Proc. 16th ACM Int. Symp. Mobile Ad Hoc Netw. Comput. (MobiHoc)*, 2015, pp. 267–276.
- [34] X. Wang, C. Yang, and S. Mao, "PhaseBeat: Exploiting CSI phase data for vital sign monitoring with commodity WiFi devices," in *Proc. 37th Int. Conf. Distrib. Comput. Syst. (ICDCS)*, 2017, pp. 1230–1239.
- [35] Y. Yang, J. Cao, X. Liu, and K. Xing, "Multi-person sleeping respiration monitoring with COTS WiFi devices," in *Proc. 15th Int. Conf. Mobile Ad Hoc Sensor Syst. (MASS)*, 2018, pp. 37–45.
- [36] Y. Zeng, Z. Liu, D. Wu, J. Liu, J. Zhang, and D. Zhang, "A multi-person respiration monitoring system using COTS WiFi devices," in *Adjunct Proc. ACM Int. Joint Conf. Pervasive Ubiquitous Comput. Int. Symp. Wearable Comput.*, 2020, pp. 195–198.
- [37] J. Liu, Y. Chen, Y. Wang, X. Chen, J. Cheng, and J. Yang, "Monitoring vital signs and postures during sleep using WiFi signals," *IEEE Internet Things J.*, vol. 5, no. 3, pp. 2071–2084, Jun. 2018.
- [38] Y. Zeng, D. Wu, R. Gao, T. Gu, and D. Zhang, "FullBreathe: Full human respiration detection exploiting complementarity of CSI phase and amplitude of WiFi signals," *Proc. ACM Interact. Mobile Wearable Ubiquitous Technol. (ACM UbiComp)*, vol. 2, no. 3, pp. 1–19, 2018.
- [39] Q. Gao, J. Tong, J. Wang, Z. Ran, and M. Pan, "Device-free multi-person respiration monitoring using WiFi," *IEEE Trans. Veh. Technol.*, vol. 69, no. 11, pp. 14083–14087, Nov. 2020.
- [40] Y. Zeng, D. Wu, J. Xiong, J. Liu, Z. Liu, and D. Zhang, "MultiSense: Enabling multi-person respiration sensing with commodity WiFi," in *Proc. ACM Interact. Mobile Wearable Ubiquitous Technol.*, vol. 4, no. 3, pp. 1–29, 2020.
- [41] J. Liu, Y. Zeng, T. Gu, L. Wang, and D. Zhang, "WiPhone: Smartphone-based respiration monitoring using ambient reflected WiFi signals," in *Proc. ACM Interact. Mobile Wearable Ubiquitous Technol.*, vol. 5, no. 1, pp. 1–19, 2021.
- [42] R. Nandakumar, S. Gollakota, and N. Watson, "Contactless sleep apnea detection on smartphones," in *Proc. 13th Annu. Int. Conf. Mobile Syst. Appl. Services (MobiSys)*, 2015, pp. 45–57.

- [43] X. Xu, J. Yu, Y. Chen, Y. Zhu, L. Kong, and M. Li, "Breathlistener: Fine-grained breathing monitoring in driving environments utilizing acoustic signals," in *Proc. 17th Annu. Int. Conf. Mobile Syst. Appl. Services (MobiSys)*, 2019, pp. 54–66.
- [44] X. Wang, R. Huang, C. Yang, and S. Mao, "Smartphone sonar-based contact-free respiration rate monitoring," *ACM Trans. Comput. Healthcare*, vol. 2, no. 2, pp. 1–26, 2021.
- [45] X. Guo, J. Liu, and Y. Chen, "FitCoach: Virtual fitness coach empowered by wearable mobile devices," in *Proc. IEEE Conf. Comput. Commun. (INFOCOM)*, 2017, pp. 1–9.
- [46] X. Sun, L. Qiu, Y. Wu, Y. Tang, and G. Cao, "SleepMonitor: Monitoring respiratory rate and body position during sleep using smartwatch," *Proc. ACM Interact. Mobile Wearable Ubiquitous Technol.*, vol. 1, no. 3, pp. 1–22, 2017.
- [47] L. Chang et al., "SleepGuard: Capturing rich sleep information using smartwatch sensing data," *Proc. ACM Interact. Mobile Wearable Ubiquitous Technol.*, vol. 2, no. 3, pp. 1–34, 2018.
- [48] B. G. Lee, B. L. Lee, and W. Y. Chung, "Smartwatch-based driver alertness monitoring with wearable motion and physiological sensor," in *Proc. 37th Annu. Int. Conf. IEEE Eng. Med. Biol. Soc. (EMBC)*, 2015, pp. 6126–6129.
- [49] T. Hao, C. Bi, G. Xing, R. Chan, and L. Tu, "MindfulWatch: A smartwatch-based system for real-time respiration monitoring during meditation," *Proc. ACM Interact. Mobile Wearable Ubiquitous Technol.*, vol. 1, no. 3, pp. 1–19, 2017.
- [50] D. Liaqat et al., "WearBreathing: Real world respiratory rate monitoring using smartwatches," *Proc. ACM Interact. Mobile Wearable Ubiquitous Technol.*, vol. 3, no. 2, pp. 1–22, 2019.
- [51] A. Havriushenko, K. Slyusarenko, and I. Fedorin, "Smartwatch based respiratory rate estimation during sleep using CNN/LSTM neural network," in *Proc. IEEE 40th Int. Conf. Electron. Nanotechnol. (ELNANO)*, 2020, pp. 584–587.
- [52] "NEULOG respiration monitor logger sensor." Dec. 2014. [Online]. Available: <http://www.neulog.com/>



Wei Liu received the Ph.D. degree from the Department of Computer Science and Technology, Donghua University, Shanghai, China, in 2021, under the supervision of S. Chang.

He is currently an Assistant Professor with the Department of Computer Science and Technology, Anhui University of Finance and Economics, Bengbu, China. His research interests include ubiquitous and pervasive computing, mobile computing/sensing, and edge computing.



Feng Li received the Ph.D. degree in information science from the Graduate School of Advanced Science and Technology, Japan Advanced Institute of Science and Technology, Ishikawa, Japan, in 2019.

He is currently an Assistant Professor with the Department of Computer Science and Technology, Anhui University of Finance and Economics, Bengbu, China. He is also a Postdoctoral Researcher with the School of Information Science and Technology, University of Science and Technology of China, Hefei, China. His research interests include audio source separation, noise reduction, and the signal processing of speech.



Yong Xu received the M.S. degree in computer application from Hefei University of Technology, Hefei, China, in 2006.

He is currently a Full Professor with the Department of Computer Science and Technology, Anhui University of Finance and Economics, Bengbu, China. His research interests include social networking, data mining, and IoT application.



Shizong Yan received the bachelor's degree from the School of Automation, Nanjing Institute of Technology, Nanjing, China, in 2014. He is currently pursuing the Ph.D. degree with the Department of Computer Science and Technology, Donghua University, Shanghai, China.

His research interests include AI system security, mobile sensing, and computing.



Shan Chang (Member, IEEE) received the Ph.D. degree in computer software and theory from Xi'an Jiaotong University, Xi'an, China, in 2013.

From 2009 to 2010, she was a Visiting Scholar with the Department of Computer Science and Engineering, Hong Kong University of Science and Technology, Hong Kong. She was also a Visiting Scholar with the BBCR Research Lab, University of Waterloo, Waterloo, ON, Canada, from 2010 to 2011. She is currently a Full Professor with the Department of Computer Science and Technology, Donghua University, Shanghai, China. Her research interests include security and privacy in mobile networks and sensor networks.

Prof. Chang is a member of the IEEE Computer Society, Communication Society, and Vehicular Technology Society.



Ye Liu received the M.S. degree from the Department of Software Engineering, Kunming University of Science and Technology, Kunming, China, in 2019. She is currently pursuing the Ph.D. degree with the School of Computer Science and Technology, Donghua University, Shanghai, China.

Her research interests include ubiquitous and pervasive computing, and privacy and security of federated learning.